



Periodic changes in the orientation of orbits and the age of the Galactic bar

E. Podzolkova^{1,2} and A. Melnik¹

¹ Sternberg Astronomical Institute, Lomonosov Moscow State University, Universitetskij pr. 13, Moscow, 119991 Russia

² Faculty of Physics, Lomonosov Moscow State University, Leninskie Gory 1–2, Moscow, 119991 Russia

Abstract. We studied the model of the Galaxy that reproduces the observed median velocity distribution derived from *Gaia* DR3 data along the Galactocentric distance, R . The model profiles of radial velocity, V_R , demonstrate an increase with a period of $P = 2.1 \pm 0.1$ Gyr and form humps at $R = 6\text{--}7$ kpc. The average amplitude of variation in the radial velocity is $A = 1.76 \pm 0.20$ km s⁻¹. The humps are supported by orbits changing orientation relative to the major axis of the bar within the range of $[-45, 45]^\circ$. The median period of variation in the angular momentum of hump-supporting orbits is $P = 1.85 \pm 0.17$ Gyr, and 71.6% of them support ring R_2 . The observed profile does not show any humps. In the model profile, humps disappear during the times 2.5 ± 0.3 and 4.5 ± 0.5 Gyr, indicating that the age of the Galactic bar must be close to one of these values. The model disk forms outer resonance rings R_1 and R_2 , which demonstrate periodic changes in their morphology with a period of $P = 2.0 \pm 0.1$ Gyr, supported by orbits trapped by the Outer Lindblad Resonance.

Keywords: Galaxy: kinematics and dynamics

DOI: 10.26119/VAK2024.084

1 Introduction

Although there is strong evidence for the existence of a bar in the Galaxy, for example, see Benjamin et al. (2005), its age is still a matter of debate. Different estimates show values ranging from 3 to 8 Gyr. The angular velocity of the bar, Ω_b , usually lies in the range 40–60 km s⁻¹ kpc⁻¹. The rotation of the bar leads to the appearance of resonances:

$$\frac{m}{n} = \frac{\kappa}{\Omega - \Omega_b}, \quad (1)$$

where m is the number of full epicyclic oscillations that a star makes during n revolutions relative to the bar, and κ is the epicyclic frequency. The conditions $\Omega = \Omega_b$, $m/n = 2/1$ and $m/n = -2/1$ determine the locations of the Corotation Radius (CR), Inner Lindblad Resonance (ILR) and Outer Lindblad Resonance (OLR), respectively. Weinberg (1994) demonstrated that stars captured by the ILR and OLR frequently exhibit periodic changes in the direction of their orbital elongation relative to the major axis of the bar.

2 Observations and the model

We selected stars with measured line-of-sight velocities from the *Gaia* DR3 catalog (Gaia Collaboration et al. 2023) that lie near the Galactic plane ($|z| < 200$ pc) and within a sector of Galactocentric angles $|\theta| < 15^\circ$. We excluded stars that have parallaxes determined with the relative error of more than 20% ($\varpi/\epsilon_\varpi < 5$) and with the renormalized error $\text{RUWE} > 1.4$. The final sample includes 9.7×10^6 objects. The solar Galactocentric distance is adopted to be $R_0 = 7.5$ kpc. We calculated the median radial (V_R) and azimuthal (V_T) velocity components in 250-pc wide bins along the distance R . The observed radial velocity profile has specific features: V_R demonstrates a plateau with $V_R \approx 5$ km s⁻¹ at the distance range of 5–7 kpc and then a smooth fall to the value of $V_R \approx -3$ km s⁻¹ at the distance $R = 8.5$ kpc (see red dashed line in Fig. 1a, b).

We studied a 2D model of the Galaxy with an analytical Ferrers bar (Athanasoula et al. 1983) that reproduces well the observed velocity profiles. The model has a flat rotation curve at the periphery and includes a bar, a bulge, a disk, and an isothermal halo. Semi-axes of the bar are $a = 3.5$ kpc and $b = 1.35$ kpc, and its mass is $M_{rmb} = 1.2 \times 10^{10} M_\odot$. The angular velocity of the bar is $\Omega_b = 55$ km s⁻¹ kpc⁻¹, which leads to the positions of the CR and OLR at $R_{\text{CR}} = 4.04$ kpc and $R_{\text{OLR}} = 7.00$ kpc, respectively. At the start of the simulation, the model disk is axisymmetric, and the non-axisymmetric component grows over 4 bar rotation periods, which corresponds to $T = 450$ Myr. Model includes 2×10^6 massless particles, and the time of

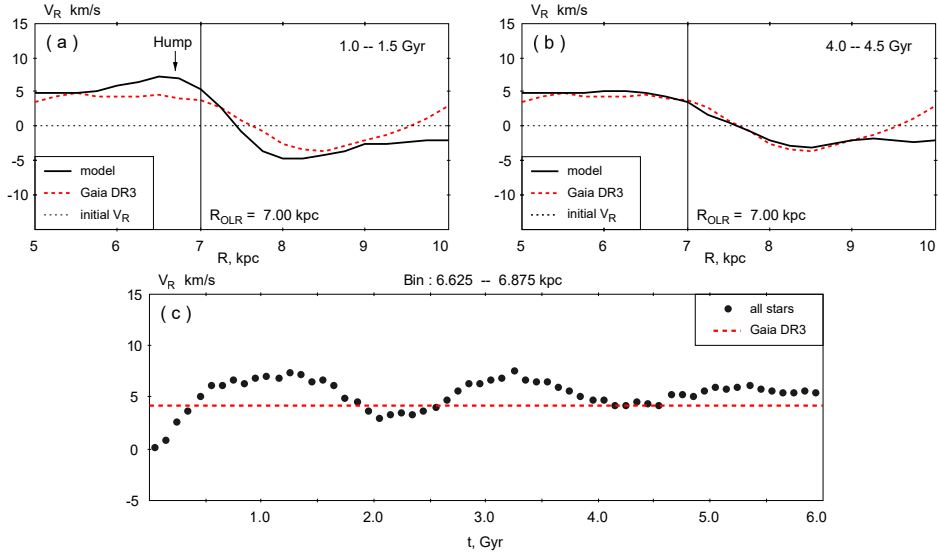


Fig. 1. The appearance of the humps on the radial velocity distribution. (a) Distribution of the median radial velocity, V_R , along the Galactocentric distance in the sector of $|\theta - \theta_\odot| < 15^\circ$, averaged over time interval of $T = 1.0 - 1.5$ Gyr. The model velocity distribution is shown by the black solid line, while the observed one is shown by the red dashed line. The model distribution shows the hump with the maximum height $1.9 \pm 0.12 \text{ km s}^{-1}$ at the distance range of $R = 6-7$ kpc. (b) The same distribution calculated for the time interval of $T = 4.0 - 4.5$ Gyr. Note the absence of the hump. (c) Median radial velocity in the bin of the Galactocentric distance of $6.625 < R < 6.875$ kpc over time (black dots). The observed velocity is shown by a red dashed line.

simulation is 6 Gyr. The position angle of the Sun relative to the major axis of the bar is adopted to be $\theta_\odot = -45^\circ$. The order of symmetry of the model is $m = 2$. For more detail, see Melnik et al. (2021).

3 Results and discussion

Figure 1a,b shows model profiles of the radial velocity compared to the observed ones for two time intervals: $T = 1.0-1.5$ Gyr and $4.0-4.5$ Gyr from the start of simulation. The model profiles were calculated in the sector of azimuthal angles $|\theta - \theta_\odot| < 15^\circ$ and averaged over the time intervals of 500 Myr. Figure 1a shows an increase in the model velocity in the distance range of 6–7 kpc. Figure 1b shows no hump. Figure 1c shows the variation in the model velocity V_R over time in a sector of maximal height of the hump: $|\theta - \theta_\odot| < 15^\circ$ and $R = 6.625-6.875$ kpc. Amplitude of V_R variations decreases with time. The values of V_R were averaged over intervals of 100 Myr. Parameters of oscillations calculated at the interval 0–6 Gyr are following:

the average amplitude $A = 1.76 \pm 0.20 \text{ km s}^{-1}$, the initial phase $\varphi = 257 \pm 5^\circ$, the average velocity is $\overline{V_R} = 5.2 \pm 0.1 \text{ km s}^{-1}$, and the period is $P = 2.1 \pm 0.1 \text{ Gyr}$.

We identified stars that support the humps on the V_R -velocity profiles. These stars appear to lie in the considered sector of the model disk and have negative radial velocities V_R , thereby reducing the median radial velocity within it. We selected a sample of 26308 stars (9% of all stars which lie both inside and outside the OLR) which change the direction of their orbital elongation relative to the major axis of the bar, θ_0 , as $0 < \theta_{01} < 45^\circ$, $-45 < \theta_{02} < 0^\circ$ and $0 < \theta_{03} < 45^\circ$ during time intervals of 0–1, 1–2 and 2–3 Gyr, respectively. The median period of variation in the angular momentum of the sample is $P = 1.85 \pm 0.17 \text{ Gyr}$, and 71.6% of orbits are elongated along the major axis of the bar and support the ring R_2 .

Figure 2a shows an example of hump-supporting orbit. It is clearly seen that at the time intervals of 0–1 and 2–3 Gyr the orbit is tilted to the right, in the direction opposite to that of the Galactic rotation, while at the interval of 1–2 Gyr it is tilted to the left. Figure 2b shows the orientation of the orbit as a function of time. The periodic character of θ_0 is well seen, as it decreases slowly from 45° , and then grows back quickly.

Figure 2c shows the variation in the beat frequency, w_{bt} . The change in the sign of w_{bt} indicates that the orbit is librating, meaning it reverses the direction of apsidal precession, and its elongation direction oscillates within a certain angle range (see Melnik & Podzolkova 2024, Eq. 9).

After excluding 26308 hump-creating stars, the humps on the V_R profiles disappear. To estimate the influence of these stars, we calculated the ratio of the amplitude A to its uncertainty, ε_A . For all stars in the considered segment, the ratio is $|A/\varepsilon_A| = 8.8$. After excluding hump-creating stars, at the fixed values of the period and phase, we obtained $A = -0.21 \pm 0.19 \text{ km s}^{-1}$ ($|A/\varepsilon_A| = 1.1$), so the amplitude becomes close to its uncertainty.

Figure 3 shows the comparison between the model and observed V_R -velocity profiles. The χ^2 function has two minima at 2.5 ± 0.3 and $4.5 \pm 0.5 \text{ Gyr}$, corresponding to the times when the model profiles have no humps. This suggests that the age of the Galactic bar must be close to 2.5 ± 0.3 or $4.5 \pm 0.5 \text{ Gyr}$ (for more details, see Melnik & Podzolkova 2024).

Melnik et al. (2023) studied periodic changes in the morphology of the inner and outer rings. The model disk forms the nuclear ring, the inner combined ring, and the outer resonance rings R_1 and R_2 . We found the morphological changes in the outer resonance rings R_1 and R_2 with a period of $P = 2.0 \pm 0.1 \text{ Gyr}$. These changes are driven by a mechanism similar to that of hump formation. The orbits, similar to the one shown in Fig. 2a, are tilted to the right during time intervals of 0–1

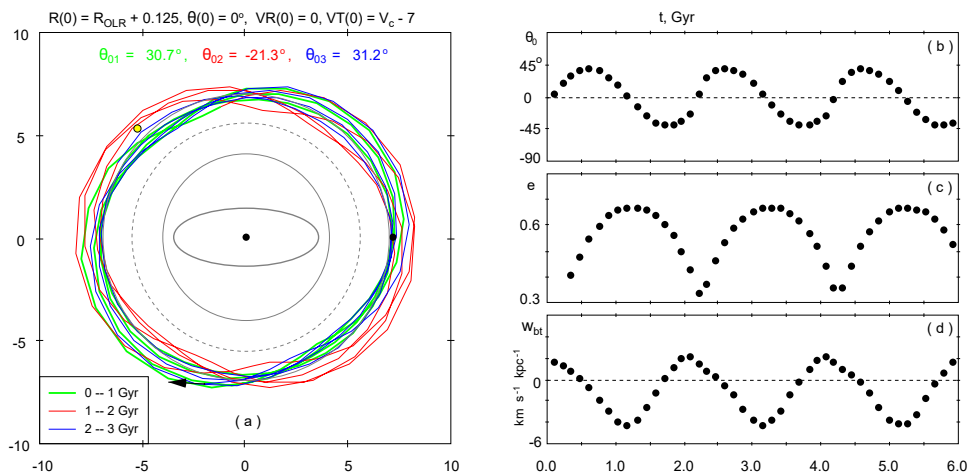


Fig. 2. An example of a hump-supporting orbit. (a) Orbit of the star in the reference frame associated with the rotating bar. The Galaxy rotates counterclockwise, but in the reference frame of the rotating bar the star rotates clockwise. The frame size is 10×10 kpc. The position of the Sun is shown by the yellow circle. At the beginning of the simulation, the star is located in the direction of the bar’s major semi-axis at a distance $R(0) = R_{\text{OLR}} + 0.125$ kpc (black circle). The initial radial and azimuthal velocities are $V_R(0) = 0$ and $V_T(0) = V_C - 7 \text{ km s}^{-1}$, where V_C is the velocity of the rotation curve. The angles θ_{01} , θ_{02} , and θ_{03} determine the orientations of the orbit with respect to the major axis of the bar at time intervals of 0–1, 1–2, and 2–3 Gyr, respectively. The bar is shown by the ellipse, the CR and the OLR — by the gray solid lines, and the $-4/1$ resonance — by the dashed line. (b) Variation in the angle θ_0 over time. (c) Changes in the eccentricity of the orbit over time. (d) Changes in the beat frequency w_{bt} over time.

and 2–3 Gyr, supporting the trailing segments of the rings, and to the left during 1–2 Gyr supporting the leading segments. The oscillation period of these orbits, $P \approx 1.91 \pm 0.01$ Gyr, is close to the period of changes in the morphology of the outer rings.

4 Summary

We studied the model of the Galaxy with an analytical Ferrers bar, which demonstrates periodic changes in the median velocities and morphology of the model disk. The radial velocity profiles form the humps with a period of $P = 2.1 \pm 0.1$ Gyr, supported by orbits whose orientations vary within the ranges $0 < \theta_{01} < 45^\circ$, $-45 < \theta_{02} < 0^\circ$ and $0 < \theta_{03} < 45^\circ$ at the time intervals of 0–1, 1–2 and 2–3 Gyr, respectively. When these orbits are excluded from the sample, the humps disappear. Similar orbits with a period of $P \approx 1.91 \pm 0.01$ Gyr support periodic changes in the morphology of

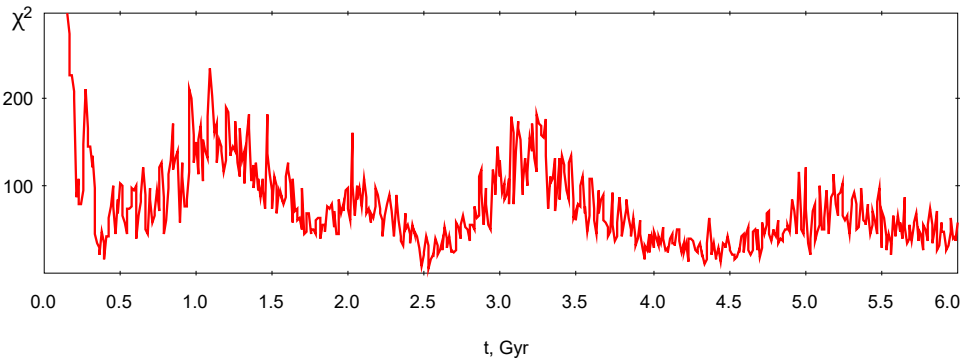


Fig. 3. Variation in the χ^2 function describing the difference between the model and observed (*Gaia* DR3) V_R velocity profiles over time. We see minima at the times 2.5 ± 0.3 and 4.5 ± 0.5 Gyr, which arise due to the disappearance of humps on the model V_R velocity profile at these times.

the outer resonance rings R_1 and R_2 . Since the observed radial velocity profile has no hump, and the model profiles have no hump at the times 2.5 ± 0.3 and 4.5 ± 0.5 Gyr, the age of the Galactic bar must be close to 2.5 ± 0.3 or 4.5 ± 0.5 Gyr.

Acknowledgements. This work has made use of data from the European Space Agency (ESA) mission *Gaia* (<https://www.cosmos.esa.int/gaia>), processed by the *Gaia* Data Processing and Analysis Consortium (DPAC, <https://www.cosmos.esa.int/web/gaia/dpac/consortium>). Funding for the DPAC has been provided by national institutions, in particular the institutions participating in the *Gaia* Multilateral Agreement. E. N. Podzolkova is a scholarship holder of the Foundation for the Advancement of Theoretical Physics and Mathematics “BASIS” (Grant No. 21-2-2-44-1).

References

- Athanassoula E., Bienayme O., Martinet L., et al., 1983, *Astronomy and Astrophysics*, 127, p. 349
 Benjamin R., Churchwell E., Babler B., et al., 2005, *Astrophysical Journal*, 630, id. L149
 Gaia Collaboration, Vallenari A., Brown A., et al., 2023, *Astronomy and Astrophysics*, 674, id. A1
 Melnik A., Dambis A., Podzolkova E., et al., 2021, *Monthly Notices of the Royal Astronomical Society*, 507, p. 4409
 Melnik A. and Podzolkova E., 2024, accepted to *Astronomy Letters*
 Melnik A., Podzolkova E., and Dambis A., 2023, *Monthly Notices of the Royal Astronomical Society*, 525, p. 3287
 Weinberg M., 1994, *Astrophysical Journal*, 420, p. 597